be calculated on the basis of assumed geometries and molecular constants. These errors will become smaller as spectroscopic measurements of the respective molecular parameters become available, permitting the calculation of more accurate thermal functions. For the molecule PdGe, a dissociation energy of $D°_0 = 252.0 \pm 10.5$ kJ mol^{-1} has previously been measured by the authors.[11] This latter value compares to the dissociation energy of 256.6 ± 12 kJ mol^{-1} reported by Peeters et al.[21] Miedema and Gingerich[22] have calculated a dissociation energy for PdGe of 308 kJ mol^{-1}, using an empirical atomic cell model. This calculated value is higher than the experimental dissociation energy, but is in reasonable agreement.

The following bond dissociation energies, in kJ mol^{-1}, between the Pd atom and the various germanium clusters, have been obtained from the experimental atomization energies:

molecule	$\Delta H_a°_0(MGe_n) - \Delta H_a°_0(Ge_n)$
PdGe	252
$PdGe_2$	340
$PdGe_3$	366

In arriving at these values the ancillary $\Delta H_a°_0(Ge_2) = 260$ kJ mol^{-1} [14] and $\Delta H_a°_0(Ge_3) = 623$ kJ mol^{-1} [13] were used.

In a previous investigation of gold-germanium clusters[13] the corresponding bond dissociation energies Au-Ge, Au-Ge_2, and Au-Ge_3 (270, 260, and 274 kJ mol^{-1}, respectively) were found to be nearly the same, which may be attributed to single-bond formation between the gold atom and germanium. As can be seen above, in the case of the palladium atom, these bond dissociation energies increase, suggesting the presence of multiple bonds between palladium and germanium.

The theoretical results for PdGe[10,11] are used to support this conclusion. The bond in PdGe is formed by interaction between a Pd atom in its $^1S(4d)^{10}$ ground term and a Ge atom in the $(4s)^2(4p\sigma)^1(4p\pi)^1$ configuration. As the atoms approach each other charge is donated from the 4dπ and 4dσ orbitals of palladium into the pσ and pπ orbitals of germanium. Back-donation leads to population in particular of the Pd 5s orbital. This behavior is similar to that calculated for PdC,[9,10] but unlike the case of PdC, the respective net charge transfer in PdGe from Pd to Ge is very small. While there are no theoretical calculations available for the $PdGe_2$ and $PdGe_3$ molecules and for germanium-gold molecules, the complex bonding behavior for PdGe shows significant d-electron participation in the formation of the bond. For gold-germanium molecules one can expect that the 5s electron of the gold atom contributes predominantly to the bond formation, while the d electrons remain localized. The observed significant increase in the bond energy per bond in $PdGe_2$ and $PdGe_3$ above that in PdGe may therefore be attributed to an increasing participation of the 4d electrons in these polyatomic molecules.

Acknowledgment. This work was supported by the National Science Foundation under Grant CHE-8709916 and the Robert A. Welch Foundation under Grant A-0387.

(21) Peeters, R.; Vander Auwera-Mahieu, A. M.; Drowart, J. *Z. Naturforsch., A* **1971**, *26*, 327.
(22) Miedema, A. R.; Gingerich, K. A. *J. Phys. B* **1979**, *12*, 2081, 2255.

Contribution from the Christopher Ingold Laboratories, University College London, 20 Gordon Street, London WC1H 0AJ, England

Infrared, Raman, Resonance Raman, and Excitation Profile Studies of $Rh_2(O_2CCH_3)_4L_2$ (L = $AsPh_3$, $SbPh_3$)†

Robin J. H. Clark* and Andrew J. Hempleman

Received June 17, 1988

The infrared, Raman, and resonance Raman spectra of the complexes $Rh_2(O_2CCH_3)_4L_2$ (L = $AsPh_3$, $SbPh_3$) have been studied and compared in detail with those of the analogous complex with L = PPh_3. The resonance Raman spectra are particularly rich, many overtone progressions being detected in each case at resonance with the axially polarized $\sigma \rightarrow \sigma^*$ transition at ca. 360 nm. The principal progression-forming mode is invariably ν_1, ν(Rh-Rh), implying a substantial geometric change along this coordinate on excitation to the σ^* state. The excitation profiles of the enhanced bands of all three complexes reach a maximum within the contour of the $\sigma \rightarrow \sigma^*$ band, which implies that there are also minor geometric changes to other coordinates on excitation to the σ^* state.

Introduction

In a previous publication on the series of complexes $Rh_2(O_2CR)_4(PPh_3)_2$, where R = H, CH_3, C_2H_5, or C_3H_7, it was shown that changes in the carboxylate alkyl group cause only a small, ca. ±7 cm^{-1}, variation in ν_1, ν(Rh-Rh), whereas the totally symmetric ν(Rh-O) vibration, ν_2, is strongly dependent on the mass of the R group.[1] Consequently, the important distinction between bands arising from the key skeletal fundamentals, ν(M-M) and ν(M-O), of dimeric tetracarboxylates can be made on the basis of sensitivity of ν(M-O) to the carboxylate alkyl group. In the present study of the complexes $Rh_2(O_2CCH_3)_4L_2$ (L = $AsPh_3$, $SbPh_3$),[2] the axial ligands only are substituted for PPh_3, in consequence of which ν_1 would be expected to change but not, to a first approximation (via the G matrix), ν_2. Thus a complementary method for distinguishing between ν_1 and ν_2 is developed. The reason for assuming that it might be possible to make the distinction between these two fundamentals on this basis is the realization that there is considerable sensitivity of ν(Mo-Mo) to the masses and nature of the axial ligands in the dimolybdenum series $Mo_2(O_2CCF_3)_4$ (398-395 cm^{-1})[3,4] and $Mo_2(O_2CCF_3)_4L_2$, where L = CH_3OH (386 cm^{-1}),[3] pyridine (368-367 cm^{-1}),[4,5] PPh_3 (377[3] or 367[6] cm^{-1}), $AsPh_3$ (375 cm^{-1}),[7] and $AsEt_3$ (368 cm^{-1}).[7] Earlier X-ray studies of the three dirhodium tetraacetate complexes[2] and Raman studies of $Rh_2(O_2CCH_3)_4(PPh_3)_2$[8] are now amplified by detailed studies of the Raman, resonance Raman, and infrared spectroscopy of the $AsPh_3$ and $SbPh_3$ complexes and,

† Tetrakis(μ-acetato)bis[(triphenylarsine)rhodium(II)](*Rh-Rh*); tetrakis(μ-acetato)bis[(triphenylstibine)rhodium(II)](*Rh-Rh*).

(1) Clark, R. J. H.; Hempleman, A. J. *Inorg. Chem.*, in press.
(2) Clark, R. J. H.; Hempleman, A. J.; Dawes, H. M.; Hursthouse, M. B.; Flint, C. D. *J. Chem. Soc., Dalton Trans.* **1985**, 1775-1780.
(3) Ketteringham, A. P.; Oldham, C. *J. Chem. Soc., Dalton Trans.* **1973**, 1067-1070.
(4) San Filippo, J., Jr.; Sniadoch, H. J. *Inorg. Chem.* **1973**, *12*, 2326-2333.
(5) Cotton, F. A.; Norman, J. G., Jr. *J. Am. Chem. Soc.* **1972**, *94*, 5697-5702.
(6) Garner, C. D.; Senior, R. G. *J. Chem. Soc., Dalton Trans.* **1975**, 1171-1174.
(7) Ribas, J.; Jugie, G.; Poilblanc, R. *Transition Met. Chem. (Weinheim, Ger.)* **1983**, *8*, 93-98.
(8) Clark, R. J. H.; Hempleman, A. J. *Inorg. Chem.* **1988**, *27*, 2225-2229.

0020-1669/89/1328-0092$01.50/0

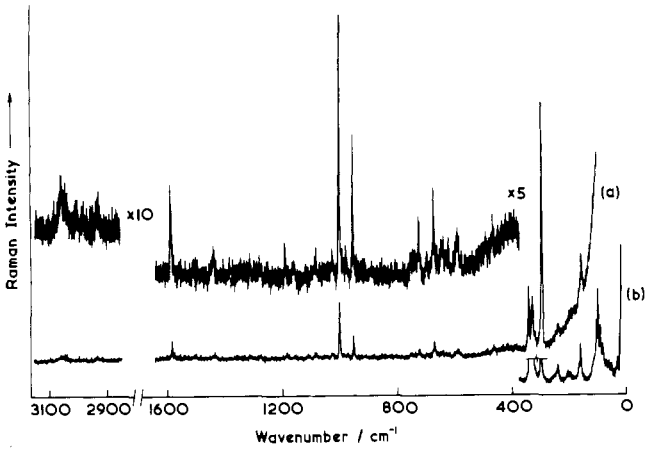

Figure 1. Raman spectra (3150–2850 and 1630–20 cm^{-1}) of $Rh_2(O_2CCH_3)_4(AsPh_3)_2$ as a KCl disk at ca. 80 K with 514.5-nm excitation. The resolution is ca. 3 cm^{-1}. The spectra were obtained (a) in the double- and (b) in the triple-monochromator modes.

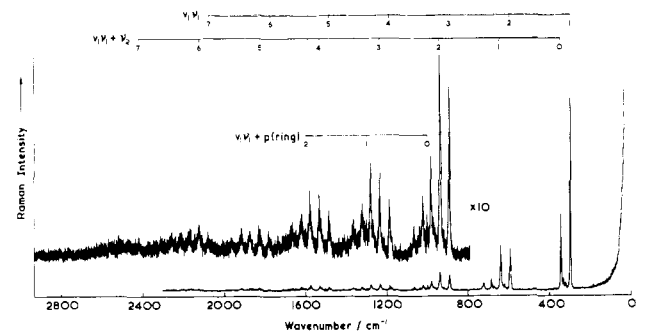

Figure 2. Resonance Raman spectrum (2900–30 cm^{-1}) of $Rh_2(O_2CCH_3)_4(AsPh_3)_2$ as a KCl disk at ca. 80 K with 350.7-nm excitation. The resolution is ca. 4 cm^{-1}.

in particular, by extensive studies of the excitation profiles of resonance-enhanced Raman bands. Analysis of such profiles can, in some cases,[9] lead to estimates for the geometric changes associated with excitation of such molecules from the ground to the resonant excited state.

Experimental Section

The complexes $Rh_2(O_2CCH_3)_4L_2$ (L = $AsPh_3$, $SbPh_3$) were prepared and analyzed as described previously.[2]

Raman spectra were recorded with a Spex 14018 (R6) spectrometer in both the double- and the triple-monochromator modes, in conjunction with Coherent CR 3000 K and CR12 lasers. Samples for Raman spectroscopy were held as KCl disks at ca. 80 K in a liquid-nitrogen cell. Infrared spectra were recorded at ca. 80 K as KCl disks (3500–500 cm^{-1}) and as pressed wax disks (660–40 cm^{-1}) at a spectral resolution of 1 cm^{-1} with a Bruker 113 V interferometer. Details of the sample preparations were identical with those used in previous studies.[8,10]

Results

The Raman (λ_0 = 514.5 nm) and resonance Raman (λ_0 = 350.7 nm) spectra of $Rh_2(O_2CCH_3)_4(AsPh_3)_2$ are given in Figures 1 and 2, respectively, while the Raman (λ_0 = 514.5 nm) and resonance Raman (λ_0 = 363.8 nm) spectra of the analogous stibine complex are given in Figures 3 and 4, respectively. Profound changes in the Raman spectra take place under resonance conditions, the spectra in these circumstances displaying very rich detail associated with the appearance of many overtone progressions. Band listings for these spectra together with the assignments are given in Tables I–IV. FTIR spectra of all three related complexes $Rh_2(O_2CCH_3)_4L_2$ (L = PPh_3, $AsPh_3$, $SbPh_3$) have also been recorded in the range 3500–40 cm^{-1}, the band maxima being listed and assigned in ref 8 (PPh_3 complex) and Table V ($AsPh_3$ and $SbPh_3$ complexes). FTIR spectra of the three complexes are shown in Figure 5 for the range 660–140 cm^{-1}.

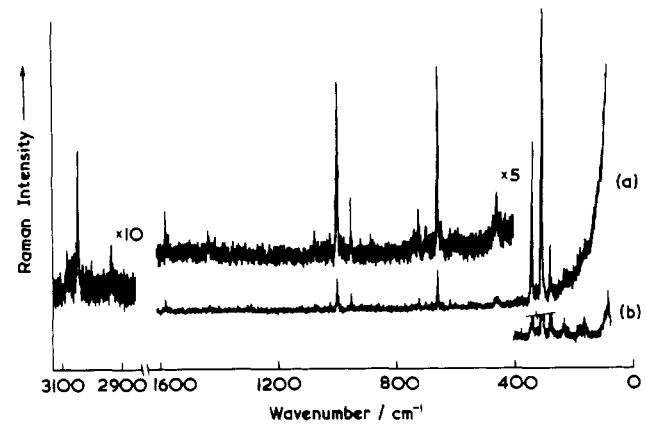

Figure 3. Raman spectra (3150–2850 and 1630–20 cm^{-1}) of $Rh_2(O_2CCH_3)_4(SbPh_3)_2$ as a KCl disk at ca. 80 K with 514.5-nm excitation. The resolution is ca. 3 cm^{-1}. The spectra were obtained (a) in the double- and (b) in the triple-monochromator modes.

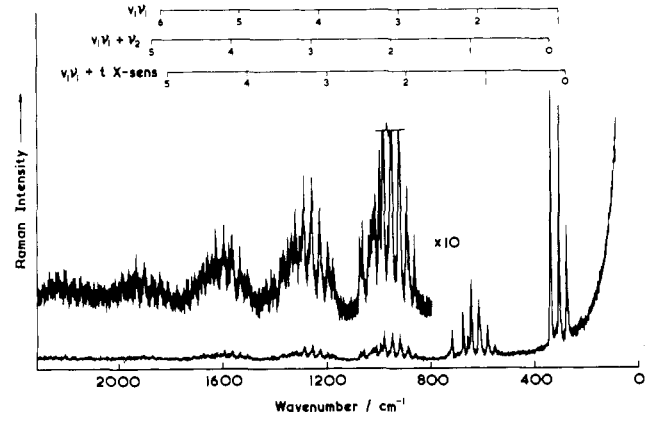

Figure 4. Resonance Raman spectrum (2300–80 cm^{-1}) of $Rh_2(O_2CCH_3)_4(SbPh_3)_2$ as a KCl disk at ca. 80 K with 363.8-nm excitation. The resolution is ca. 6.5 cm^{-1}.

Table I. Wavenumbers/cm^{-1} of Bands Observed in the Raman Spectrum[a] of $Rh_2(O_2CCH_3)_4(AsPh_3)_2$ at ca. 80 K

$\tilde{\nu}$	assgnt	$\tilde{\nu}$	assgnt[b]
30 w		630 vw	out-of-plane ρ_w(COO)
54 vw, sh		641 vw	$\nu_1 + \nu_2$
62 vw, sh		670 w	r X-sens
71 vw, sh		695 vw	v ϕ(C–C)
83 w, sh		723 vw	δ(OCO)
93 m, sh		745 vw	f γ(C–H)
103 m		951 w	ν(C–C)
117 w, sh		1000 m	p-ring
160 m		1025 vw	b β(C–H)
167 w, sh		1080 vw	q X-sens
199 vw	x X-sens	1156 vw	c β(C–H)
207 vw		1186 vw	a β(C–H)
241 w	u X-sens	1275 vw	e β(C–H)
251 vw, sh		1310 vw	v + s
297 vw	ν_1, ν(Rh–Rh)	1434 vw	n ν(C–C)
321 w, sh	ν(Rh–O)	1506 vw	
331 m	t X-sens	1573 vw	l ν(C–C)
343 m	ν_2, ν(Rh–O)	1583 w	k ν(C–C)
465 vw	y X-sens	2932 vw	ν(C–H) acetate
489 vw		3044 vw	ν(C–H) aromatic
588 vw	in-plane ρ_r(COO)	3060 vw	
617 vw	s α(C–C–C)		

[a] 514.5-nm excitation. [b] Mode lettering according to Whiffen.[12]

Discussion

The complexes $Rh_2(O_2CCH_3)_4L_2$ (L = PPh_3, $AsPh_3$, $SbPh_3$) all have strong absorption bands ($\epsilon_{max} \sim 4 \times 10^4$ M^{-1} cm^{-1}) in the near-ultraviolet region, at 376, 352, and 361 nm for L = PPh_3, $AsPh_3$, and $SbPh_3$, respectively. This band is known to be axially

(9) Clark, R. J. H.; Dines, T. J. *Angew. Chem., Int. Ed. Engl.* **1986**, *25*, 131–158.
(10) Clark, R. J. H.; Hempleman, A. J.; Tocher, D. A. *J. Am. Chem. Soc.* **1988**, *110*, 5968–5972.

Table II. Wavenumbers/cm^{-1} of Bands Observed in the Resonance Raman Spectrum[a] of $Rh_2(O_2CCH_3)_4(AsPh_3)_2$ at ca. 80 K

$\tilde{\nu}$	assgnt	$\tilde{\nu}$	assgnt
297 vs	ν_1, ν(Rh–Rh)	1297 vw	ν_1 + p-ring
321 w	ν(Rh–O)	1319 vw	$2\nu_1$ + δ(OCO)
332 w	t X-sens	1360 vw	ν_1 + ν_2 + δ (OCO)
342 m	ν_2, ν(Rh–O)	1410 vw	$2\nu_2$ + δ(OCO)
476 vw	y X-sens	1434 vw	n ν(C–C)
593 m	$2\nu_1$	1471 vw	
619 vw	ν_1 + 321	1481 vw	$5\nu_1$
626 vw, sh	ν_1 + t X-sens	1516 vw, sh	
639 m	ν_1 + ν_2	1527 vw	$4\nu_1$ + ν_2
670 w	r X-sens	1571 w	$3\nu_1$ + $2\nu_2$/l ν(C–C)
684 w	$2\nu_2$	1582 vw	k ν(C–C)
723 w	δ(OCO)	1594 vw	$2\nu_1$ + p-ring
728 vw, sh		1615 vw	$3\nu_1$ + δ(OCO)
771 vw	ν_1 + y X-sens	1658 vw	$2\nu_1$ + ν_2 + δ(OCO)
890 w	$3\nu_1$	1706 vw	ν_1 + $2\nu_2$ + δ(OCO)
915 vw	$2\nu_1$ + 321	1730 vw	ν_1 + n ν(C–C)
922 vw	$2\nu_1$ + t X-sens	1776 vw	$6\nu_1$
935 w	$2\nu_1$ + ν_2	1822 vw	$5\nu_1$ + ν_2
967 vw	ν_1 + r X-sens	1868 vw, br	$4\nu_1$ + $2\nu_2$
981 w	ν_1 + $2\nu_2$	1911 vw, br	$4\nu_1$ + δ(OCO)
1000 w	p-ring	1955 vw, br	$3\nu_1$ + ν_2 + δ(OCO)
1019 vw	ν_1 + δ(OCO)	1997 vw	$2\nu_1$ + $2\nu_2$ + δ(OCO)
1026 vw	$3\nu_2$/b β(C–H)	2073 vw, br	$7\nu_1$
1037 vw	ρ(CH_3)	2117 vw, br	$6\nu_1$ + ν_2
1065 vw	ν_2 + δ(OCO)	2162 vw, br	$5\nu_1$ + $2\nu_2$
1081 vw	q X-sens	2207 vw, br	$5\nu_1$ + δ(OCO)
1154 vw	c β(C–H)	2254 vw, br	$4\nu_1$ + ν_2 + δ(OCO)
1176 vw		2300 vw, br	$3\nu_1$ + $2\nu_2$ + δ(OCO)
1186 w	$4\nu_1$/a β(C–H)	2412 vw, br	$7\nu_1$ + ν_2
1232 w	$3\nu_1$ + ν_2	2460 vw, br	$6\nu_1$ + $2\nu_2$
1266 vw	$2\nu_1$ + r X-sens	2501 vw, br	$6\nu_1$ + δ(OCO)
1276 w	$2\nu_1$ + $2\nu_2$		

[a] 356.4-nm excitation.

Table III. Wavenumbers/cm^{-1} of Bands Observed in the Raman Spectrum[a] of $Rh_2(O_2CCH_3)_4(SbPh_3)_2$ at ca. 80 K

$\tilde{\nu}$	assgnt	$\tilde{\nu}$	assgnt
27 w		660 w	r X-sens
47 vw		677 vw	$2\nu_2$
64 vw		700 vw	v ϕ(C–C)
83 m		724 w	δ(OCO)
93 w, sh		736 vw	f γ(C–H)
160 vw		915 vw	i γ(C–H)
174 vw	x X-sens	952 w	ν(C–C)
183 vw		999 w	p-ring
217 vw, sh		1022 vw	b β(C–H)
229 vw	u X-sens	1070 vw	q X-sens
266 vw, sh	t X-sens	1162 vw	c β(C–H)
277 m		1190 vw	a β(C–H)
306 vs	ν_1, ν(Rh–Rh)	1431 vw	n ν(C–C)
322 vw	ν(Rh–O)	1569 vw, sh	l ν(C–C)
339 m	ν_2, ν(Rh-O)	1580 vw	k ν(C–C)
460 vw	y X-sens	2930 vw	ν(C–H) acetate
616 vw	s α(C-C-C)	3041 vw	ν(C–H) aromatic
646 vw	ν_1 + ν_2	3075 vw	

[a] 514.5-nm excitation.

polarized in the case of the triphenylphosphine complex[8,11] and is considered to arise from a $\sigma(Rh_2,RhL) \rightarrow \sigma^*(Rh_2)$ transition. Raman spectra taken at resonance with it are thus expected to display progressions in ν(Rh–Rh) because of the substantial change in Rh–Rh bond order associated with such a transition.[9]

The resonance Raman spectrum of $Rh_2(O_2CCH_3)_4(AsPh_3)_2$ (Figure 2) is dominated by a seven-membered progression in a band at 297 cm^{-1}, denoted ν_1, which is assigned to ν(Rh–Rh) by analogy with corresponding assignments for $Rh_2(O_2CCH_3)_4(PPh_3)_2$.[8,11] In addition to the $\upsilon_1\nu_1$ progression, ν_1 also acts as the progression-forming mode in nine further progressions to at least υ_1 = 2, notably $\upsilon_1\nu_1$ + ν_2 (to υ_1 = 7), where ν_2 is the totally symmetric ν(Rh–O) mode at 342 cm^{-1}. Most of the enabling modes for these progressions are ones that involve large donor-atom amplitudes, i.e. the X-sensitive vibrations[12] (Table VI). The dominance of ν_1 in these progressions implies that, as expected, the principal structural change on excitation to the ca. 360 nm

Table IV. Wavenumbers/cm^{-1} of Bands Observed in the Resonance Raman Spectrum[a] of $Rh_2(O_2CCH_3)_4(SbPh_3)_2$ at ca. 80 K

$\tilde{\nu}$	assgnt	$\tilde{\nu}$	assgnt
225 vw	u X-sens	1228 w	$4\nu_1$
270 w, sh	t X-sens	1258 w	$3\nu_1$ + ν_2
277 m		1268 vw, sh	$2\nu_1$ + r X-sens
307 vs	ν_1, ν(Rh–Rh)	1289 w	$2\nu_1$ + $2\nu_2$
316 w	ν(Rh–O)	1305 vw	ν_1 + p-ring
339 vs	ν_2, ν(Rh–O)	1320 vw	ν_1 + $3\nu_2$
554 w	2(t X-sens)	1335 vw	$2\nu_1$ + δ(OCO)
575 w, sh	ν_1 + t X-sens	1350 vw	$4\nu_2$
583 m	ν_1 + t X-sens	1368 vw	ν_1 + ν_2 + δ(OCO)
615 m	$2\nu_1$	1380 vw	ν_1 + q X-sens
645 m	ν_1 + ν_2	1400 vw	$2\nu_2$ + δ(OCO)
659 w	r X-sens	1415 vw	ν_2 + q X-sens
678 m	$2\nu_2$	1435 vw	n ν(C–C)
699 vw	v ϕ(C–C)	1505 vw	$4\nu_1$ + t X-sens
723 m	δ(OCO)	1515 vw	
860 vw	ν_1 + 2(t X-sens)	1535 vw	$5\nu_1$
880 w	$2\nu_1$ + t X-sens	1566 vw	$4\nu_1$ + ν_2
890 w	$2\nu_1$ + t X-sens	1580 vw	k ν(C–C)
921 w	$3\nu_1$	1596 vw	$3\nu_1$ + $2\nu_2$
952 w	$2\nu_1$ + ν_2/ν(C–C)	1627 vw	$2\nu_1$ + $3\nu_2$
964 vw	ν_1 + r X-sens	1642 vw	$3\nu_1$ + δ(OCO)
983 w	ν_1 + $2\nu_2$	1658 vw	ν_1 + $4\nu_2$
998 w	p-ring	1673 vw	$2\nu_1$ + ν_2 + δ(OCO)
1016 w	$3\nu_2$	1740 vw	ν_1 + n ν(C–C)
1022 w	b β(C–H)	1780 vw	$4\nu_1$ + 2(t X-sens)
1029 w	ν_1 + δ(OCO)	1812 vw	$5\nu_1$ + t X-sens
1038 w	ρ(CH_3)	1844 vw	$6\nu_1$
1062 w	ν_2 + δ(OCO)	1874 vw	$5\nu_1$ + ν_2
1075 w	q X-sens	1902 vw	$4\nu_1$ + $2\nu_2$
1165 vw	c β(C–H)	1933 vw	$3\nu_1$ + $3\nu_2$
1176 vw		1962 vw	
1197 vw	$3\nu_1$ + t X-sens	1990 vw	

[a] 363.8-nm excitation.

Table V. Wavenumbers/cm^{-1} of Bands Observed in the Far-Infrared (660–40 cm^{-1}) Spectra of $Rh_2(O_2CCH_3)_4L_2$ (L = $AsPh_3$, $SbPh_3$) at ca. 80 K

$AsPh_3$		$SbPh_3$	
$\tilde{\nu}$	assgnt	$\tilde{\nu}$	assignt
627 w	out-of-plane ρ_w(COO)	660 w	r X-sens
624 w		658 w	
617 vw	s α(C–C–C)	624 w	out-of-plane ρ_w(COO)
616 vw		616 vw	s α(C–C–C)
592 vw	in-plane ρ_r(COO)	615 vw	
588 vw		592 vw	in-plane ρ_r(COO)
476 w	y X-sens	588 vw	
470 m		457 w	y X-sens
466 w		452 w	
461 vw		442 w	
403 vw	w ϕ(C–C)	397 vw	w ϕ(C–C)
398 vw		393 vw	
386 w	ν(Rh–O)	391 vw	
378 w		383 w	ν(Rh–O)
333 vw, sh		379 w	
330 w	t X-sens	322 w	
327 w		280 w	t X-sens
323 w	ν(Rh–O)	270 w	
318 w	t X-sens	267 w	
241 vw	u X-sens	250 vw	
205 vw	δ(O–Rh–O)/ δ(Rh–Rh–O) or x X-sens	231 vw	u X-sens
		222 vw	
		216 vw	
112 vw		203 vw	δ(O–Rh–O) or δ(Rh–Rh–O)
		184 vw	x X-sens
		173 vw	
		157 vw	

(11) Clark, R. J. H.; Hempleman, A. J.; Flint, C. D. *J. Am. Chem. Soc.* **1986**, *108*, 518–520.

(12) Whiffen, D. H. *J. Chem. Soc.* **1956**, 1350–1356.

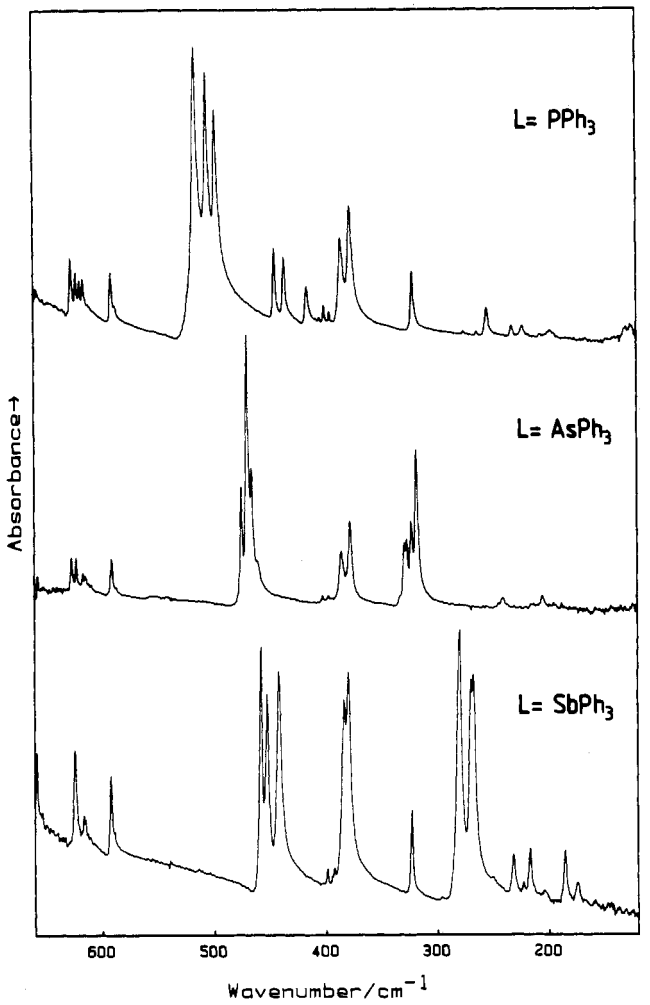

Figure 5. FTIR spectra (660–140 cm^{-1}) of $Rh_2(O_2CCH_3)_4L_2$, where L = PPh_3, $AsPh_3$, or $SbPh_3$, as wax disks at ca. 80 K.

state is along the Rh–Rh coordinate.[9]

The resonance Raman spectrum of $Rh_2(O_2CCH_3)_4(SbPh_3)_2$ (Figure 4) likewise contains many progressions. The principal progression-forming mode (at 307 cm^{-1}) is again denoted ν_1 and attributed to ν(Rh–Rh); it forms part of at least eight progressions. The band attributed to ν_2, the totally symmetric ν(Rh–O) mode, is comparable in intensity to ν_1 and occurs at 339 cm^{-1}, barely 3 cm^{-1} below that for the analogous arsine complex. Such behavior—that of virtual insensitivity to axial substitution—would be expected for a ν(Rh–O) mode owing to the very close structural similarity between all the complexes and, in particular, to the close similarity between their Rh–O bond lengths (2.045–2.040 Å).[2] It is significant in this context that the infrared-active ν(Rh–O) mode of lowest wavenumber (Table V) is likewise insensitive to axial substitution (322 ± 1 cm^{-1}) for all three complexes, L = PPh_3,[8] $AsPh_3$, or $SbPh_3$.

The assignment of ν_1 in each case is strengthened by the clear existence of the expected reciprocal relationship between ν_1 and the Rh–Rh bond length; viz., for L = PPh_3, $AsPh_3$, and $SbPh_3$, ν_1 increases in the order 289, 297, and 307 cm^{-1} while r(Rh–Rh) decreases in the order 2.4505,[13] 2.427,[2] and 2.421 Å,[2] respectively.

The most surprising feature of the resonance Raman spectra of these complexes is the substantial involvement of so many X-sensitive modes in combination band progressions with ν_1 and, in some cases, also with ν_2. More and longer progressions appear for the triphenylarsine and triphenylstibine complexes than for the triphenylphosphine complex (Table VI). This may be partly connected with the fact that phosphorus is the lightest of the three axial donor atoms considered, a situation that allows it to have a larger amplitude of vibration than is the case for the other two donor atoms, and partly connected with decreased coupling between donor atom and phenyl group on angular grounds; cf.

(13) Christoph, G. G.; Halpern, J.; Khare, G. P.; Koh, Y. B.; Romanowski, C. *Inorg. Chem.* **1981**, *20*, 3029–3037.

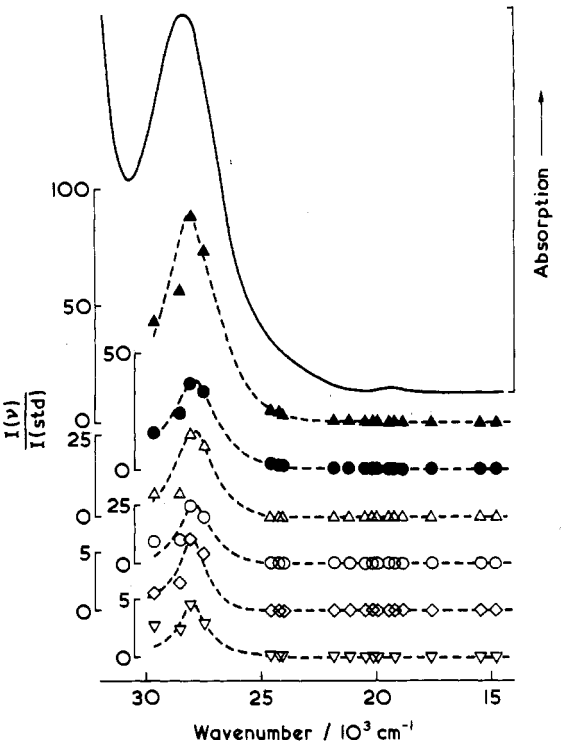

Figure 6. Excitation profiles of ν_1 (▲), ν_2 (●), $2\nu_1$ (△), $\nu_1 + \nu_2$ (○), $2\nu_2$ (◇), and δ(OCO) (▽) for $Rh_2(O_2CCH_3)_4(AsPh_3)_2$ at ca. 80 K, together with the transmission electronic spectrum recorded as a KCl disk at ca. 20 K.

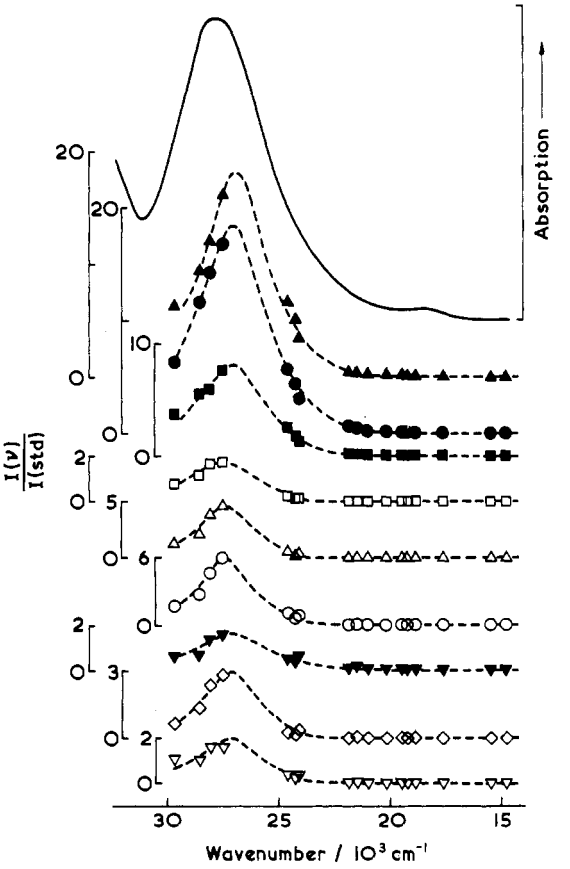

Figure 7. Excitation profiles of ν_1 (▲), ν_2 (●), t X-sens (■), $\nu_1 + $ t X-sens (□), $2\nu_1$ (△), $\nu_1 + \nu_2$ (○), r X-sens (▼), $2\nu_2$ (◇) and δ(OCO) (▽) for $Rh_2(O_2CCH_3)_4(SbPh_3)_2$, together with the transmission electronic spectrum recorded as a KCl disk at ca. 20 K.

Table VI. Principal Combination Band Progressions Observed in the Resonance Raman Spectra of $Rh_2(O_2CCH_3)_4L_2$ (L = PPh_3, $AsPh_3$, $SbPh_3$)

ν_1 band progressions		ν_2 band progressions	
from	to	from	to
	PPh_3 Complex[8]		
$\upsilon_1\nu_1$	$\upsilon_1 = 4$	$\upsilon_2\nu_2$	$\upsilon_2 = 2$
$\upsilon_1\nu_1 + \nu_2$	$\upsilon_1 = 3$		
$\upsilon_1\nu_1 + 2\nu_2$	$\upsilon_1 = 2$		
$\upsilon_1\nu_1$ + q X-sens	$\upsilon_1 = 2$		
$\upsilon_1\nu_1$ + 305	$\upsilon_1 = 2$		
	$AsPh_3$ Complex		
$\upsilon_1\nu_1$	$\upsilon_1 = 7$	$\upsilon_2\nu_2$	$\upsilon_2 = 3$
$\upsilon_1\nu_1 + \nu_2$	$\upsilon_1 = 7$	$\upsilon_2\nu_2 + \nu_1$	$\upsilon_2 = 2$
$\upsilon_1\nu_1 + \delta$(OCO)	$\upsilon_1 = 6$	$\upsilon_2\nu_2 + \delta$(OCO)	$\upsilon_2 = 2$
$\upsilon_1\nu_1 + 2\nu_2$	$\upsilon_1 = 6$		
$\upsilon_1\nu_1 + \nu_2 + \delta$(OCO)	$\upsilon_1 = 4$		
$\upsilon_1\nu_1 + 2\nu_2 + \delta$(OCO)	$\upsilon_1 = 3$		
$\upsilon_1\nu_1$ + p-ring	$\upsilon_1 = 2$		
$\upsilon_1\nu_1$ + r X-sens	$\upsilon_1 = 2$		
$\upsilon_1\nu_1$ + t X-sens	$\upsilon_1 = 2$		
$\upsilon_1\nu_1$ + 321	$\upsilon_1 = 2$		
	$SbPh_3$ Complex		
$\upsilon_1\nu_1$	$\upsilon_1 = 6$	$\upsilon_2\nu_2$	$\upsilon_2 = 4$
$\upsilon_1\nu_1 + \nu_2$	$\upsilon_1 = 5$	$\upsilon_2\nu_2 + \nu_1$	$\upsilon_2 = 4$
$\upsilon_1\nu_1$ + t X-sens	$\upsilon_1 = 5$	$\upsilon_2\nu_2 + \delta$(OCO)	$\upsilon_2 = 2$
$\upsilon_1\nu_1 + 2\nu_2$	$\upsilon_1 = 4$		
$\upsilon_1\nu_1 + 3\nu_2$	$\upsilon_1 = 3$		
$\upsilon_1\nu_1 + \delta$(OCO)	$\upsilon_1 = 3$		
$\upsilon_1\nu_1$ + r X-sens	$\upsilon_1 = 2$		
$\upsilon_1\nu_1 + \nu_2 + \delta$(OCO)	$\upsilon_1 = 2$		

∠CMC in the coordinated ligand, which decreases in the order 103.2, 101.5, and 99.7° for M = P,[13] As,[2] and Sb,[2] respectively. The principal X-sensitive (X-sens) modes involved in this coupling are the p, q, r, t, and y modes. The δ(OCO) mode is, interestingly, also involved in combination band progressions with both ν_1 and ν_2, indicating that slight structural changes on $\sigma \rightarrow \sigma^*$ excitation must occur throughout the acetate rings.

Excitation profiles have been constructed for the ν_1, ν_2, $2\nu_1$, $\nu_1 + \nu_2$, $2\nu_2$, and δ(OCO) bands of $Rh_2(O_2CCH_3)_4(AsPh_3)_2$ and for the ν_1, ν_2, t X-sens, ν_1 + t X-sens, $2\nu_1$, $\nu_1 + \nu_2$, r X-sens, $2\nu_2$, and δ(OCO) bands of $Rh_2(O_2CCH_3)_4(SbPh_3)_2$ (Figures 6 and 7). As is the case for the excitation profiles of the analogous triphenylphosphine complex,[8] all the Raman bands maximize under the contour of the resonant electronic band. Depolarization ratios were obtained on resonance for the ν_1 band of $Rh_2(O_2CCH_3)_4(AsPh_3)_2$ and for the ν_1, ν_2, and t X-sens bands of $Rh_2(O_2CCH_3)_4(SbPh_3)_2$; all were close to 1/3, which confirms the axial nature of the resonant transition.[9,14] These results indicate that, although the principal geometric change on excitation is along the Rh–Rh coordinate, there are small consequential geometric changes along many other coordinates—changes associated not only with the acetate rings but also, and more surprisingly, with X-sensitive modes of the phenyl rings. It is hoped, in future analyses, to be able to quantify these changes.

The principal progression-forming mode (ν_1) in each resonance Raman spectrum is almost harmonic; thus, for the $AsPh_3$ complex, $\omega_1 = 297.2$ cm^{-1} and $x_{11} = -0.16$ cm^{-1} while, for the $SbPh_3$ complex, $\omega_1 = 307$ cm^{-1} and $x_{11} = 0.0$ cm^{-1}. This mirrors the similar behavior displayed by the analogous PPh_3 complex.[8]

Acknowledgment. We thank the SERC and the ULIRS for financial support.

Registry No. $Rh_2(O_2CCH_3)_4(AsPh_3)_2$, 34767-18-5; $Rh_2(O_2CCH_3)_4(SbPh_3)_2$, 100237-77-2.

Supplementary Material Available: Tables VIII and IX, containing full band listings and assignments for the infrared spectra of the $AsPh_3$ and $SbPh_3$ complexes (4 pages). Ordering information is given on any current masthead page.

(14) Mortensen, O. S.; Hassing, S. In *Advances in Infrared and Raman Spectroscopy*; Clark, R. J. H., Hester, R. E., Eds.; Heyden: London, 1980; Vol. 6, pp 1-60.

Contribution from the Departments of Chemistry, NREC College, Khurja-203131 (UP), India, and Indian Institute of Technology, Hauz Khas, New Delhi-110016, India

Magnetic and Spectroscopic Characterization of the High-Spin ($^6A_1$) ⇌ Low-Spin ($^2T_2$) Transition in an Iron(III) Complex of Pyridoxal Thiosemicarbazone

Madan Mohan,*[,†] Puranam H. Madhuranath,[†] Alok Kumar,[†] Munesh Kumar,[†] and Narendra K. Jha[‡]

Received April 8, 1988

The preparation and characterization of the new discontinuous ferric spin-crossover complex $[Fe(HL)_2]Cl$ and the hydrated low-spin form of the complex $[Fe(HL)_2]Cl\cdot 2H_2O$ are reported. In these complexes HL^- is the deprotonated form of pyridoxal thiosemicarbazone (H_2L) acting as an ONS tridentate ligand. The magnetic moments for the spin-crossover complex show a thermal hysteresis, where with sample cooling the transition temperature is 245 K and with sample heating it is 256 K. Variable-temperature ^{57}Fe Mössbauer and EPR data also provide evidence for the presence of a first-order phase transition in this complex. It is most likely that the cooperative (first-order) nature of this transition is due to the extended coupling of ferric complexes through intermolecular hydrogen-bonding interactions. EPR spectra of the two complexes in this study show that both have a singly occupied d_{xy} orbital in the ground Kramers doublet.

Introduction

Thermally driven transitions between high-spin and low-spin ground states in iron compounds have recently been the subject of numerous investigations.[1-4] It has been demonstrated that transitions of the type high spin ⇌ low spin may exhibit either an essentially discontinuous or a more gradual behavior.[4-6] The discontinuous spin-crossover transformations have been shown, on the basis of heat capacity measurements,[7-9] to be thermodynamically first-order.[10] Moreover, the observation of hysteresis[4] has been employed as an indication of the first-order character of the abrupt spin transformations. Recently, variable-temperature X-ray diffraction measurements have also revealed that discon-

[†] NREC College.
[‡] Indian Institute of Technology.

(1) König, E.; Ritter, G.; Irler, W.; Goodwin, H. A. *J. Am. Chem. Soc.* **1980**, *102*, 4681.
(2) König, E.; Ritter, G.; Kulshreshtha, S. K.; Nelson, S. M. *J. Am. Chem. Soc.* **1983**, *105*, 1924.
(3) Purcell, K. F.; Edwards, M. P. *Inorg. Chem.* **1981**, *23*, 2620.
(4) Gütlich, P. *Struct. Bonding (Berlin)* **1981**, *44*, 83.
(5) Goodwin, H. A. *Coord. Chem. Rev.* **1976**, *18*, 293.
(6) Martin, R. L.; White, A. H. *Transition Met. Chem. (Weinheim, Ger.)* **1968**, *4*, 113.
(7) Sorai, M.; Seki, S. *J. Phys. Soc. Jpn.* **1972**, *33*, 575.
(8) Sorai, M.; Seki, S. *J. Phys. Chem. Solids* **1974**, *35*, 555.
(9) Shipilov, V. I.; Zelentsov, V. V.; Zhadanov, V. M.; Turdakin, V. A. *JETP Lett. (Engl. Transl.)* **1974**, *19*, 294.

0020-1669/89/1328-0096$01.50/0